RSC Advances

PAPER

View Article Online
View Journal | View Issue

Cite this: *RSC Adv.*, 2017, **7**, 52955

Novel rod-Y_2O_3:Eu^{3+}@0.01YVO_4:Eu^{3+} with open core/shell nanostructure and "off-and-on" fluorescent performance†

Nianchen Han,[a] Xueshan Gao,[a] Guang Lu,[a] Daiwen Zeng,[a] Xia Wan,[a] Shaolong Tie*[a] and Sheng Lan*[b]

Received 11th August 2017
Accepted 9th November 2017

DOI: 10.1039/c7ra08905h

rsc.li/rsc-advances

Herein, we develop a novel sensitive fluorescent probe with an open core/shell nanostructure (OCSNS), rod-Y_2O_3:Eu^{3+}@0.01YVO_4:Eu^{3+}, in which a YVO_4:Eu^{3+} shell with a thickness of less than 5 nm partially covers an anisotropic core of rod-Y_2O_3:Eu^{3+}. The photo-luminescent performance of the OCSNS is sensitive to trace ions or molecules. High-resolution transmission electron microscopy (HR-TEM) observations clearly confirm that this OCSNS has an open quantum shell of YVO_4:Eu^{3+}. In contrast to closed core Y_2O_3:Eu^{3+}@shell YVO_4:Eu^{3+}, which has only one excitation band peaking at ~308 nm, this novel nanostructure has a wide-wavelength excitation response that can be decomposed into two components centered at ~254 and ~280 nm, which stem from open core rod-Y_2O_3:Eu^{3+} and the YVO_4:Eu^{3+} quantum shell, respectively. As expected, this OCSNS shows "off-and-on" fluorescence properties due to the strong surface effect of this open quantum shell: it is "off" when detecting trace Cu(II) ions and "on" when detecting trace amino acids, at levels as low as 10^{-8} mol L^{-1}. Hence, rod-Y_2O_3:Eu^{3+}@0.01YVO_4:Eu^{3+} could be an excellent candidate for sensitive fluorescent probes, showing similar performance to most quantum dots for the detection of ions and molecules. Moreover, it is both easier to fabricate and more stable than quantum dots.

1. Introduction

Rare-earth-doped nano-phosphors have unique properties and applications in many fields, such as white light-emitting diodes, field emission displays, and general fluorescence lamps.[1–7] They are highly popular among researchers and are gaining increasing importance in our daily lives. Y_2O_3:Eu^{3+} and YVO_4:Eu^{3+} are well-known red-emitting phosphors. Y_2O_3:Eu^{3+} shows excellent luminescent performance with high brightness, color purity, and stability.[5,8] YVO_4:Eu^{3+} also shows prominent luminescent performance owing to the strong $^5D_0$–$^7F_2$ transition due to the efficient energy transfer from VO_4^{3-} to Eu^{3+}, which provides a high quantum yield of photoluminescence (PL $q \approx 70\%$).[9,10] Rare-earth-doped nanocomposites with core/shell structures have been investigated by many researchers in attempts to obtain outstanding luminescent performance: examples with close and continuous shells on their cores include Y_2O_3:Eu^{3+}@SiO_2,[11] $CePO_4$:Tb/$LaPO_4$,[12] SiO_2@YVO_4:Dy^{3+}/Sm^{3+},[13] γ-Fe_2O_3@YVO_4:Eu^{3+},[14] and Y_2O_3:Eu^{3+}@SiO_2@YVO_4:Eu^{3+}.[15]

However, these reported nanostructures had fully coated shells, and therefore showed independent shell-only or core-only PL properties on energy transfer from the shell (or core) to the core (or shell). It is reasonable to assume that their lifetimes in both the core and shell depended on the $^5D_0$–$^7F_2$ transitions in the Eu^{3+} ions, giving different results for each system.[15] The preparation processes for obtaining these core–shell nanostructures were complex; furthermore, their fluorescences were not significantly affected by trace surrounding molecules and ions, as shown by the limited variation in the before-and-after fluorescence intensities. Therefore, these nanomaterials generally cannot be used as fluorescent probes.

Recently, quantum dots (QDs) have drawn great attention because of their unique physical and chemical properties and potential applications.[16] These nanoparticles have been employed in diverse applications such as light-absorbing components of solar cells[17–19] and light-emitting components of LEDs and lasers,[20] especially as fluorescent probes for trace

[a]College of Chemistry & Environment, South China Normal University, Guangzhou Key Laboratory of Materials for Energy Conversion and Storage, Guangzhou, Guangdong, 510006, China. E-mail: tiesl@scnu.edu.cn

[b]College of Information & Optoelectronic Science and Engineering, South China Normal University, Guangdong Provincial Key Laboratory of Nanophotonic Functional Materials and Devices, Guangzhou, 510006, China. E-mail: slan@scnu.edu.cn

† Electronic supplementary information (ESI) available: SEM image, HR-TEM image and PL spectra of Y_2O_3:Eu^{3+}@0.4YVO_4:Eu^{3+}; fluorescence response of pure Y_2O_3:Eu^{3+}, pure YVO_4:Eu^{3+}, Y_2O_3:Eu^{3+} and 0.01YVO_4:Eu^{3+}, Y_2O_3:Eu^{3+}@0.4YVO_4:Eu^{3+} in the presence of increasing concentration of Cu^{2+}; fluorescence response of rod-Y_2O_3:Eu^{3+}@0.01YVO_4:Eu^{3+} in the presence of increasing concentration of Cu^{2+}; fluorescence response of rod-Y_2O_3:Eu^{3+}@0.01YVO_4:Eu^{3+}–Cu^{2+} (10^{-8} mol L^{-1}) in the presence of increasing concentration of glutamic acid and leucine. See DOI: 10.1039/c7ra08905h

detection of some molecules and ions.[21] "Off-and-on" fluorescent probes are generally composed of many kinds of QDs and have attracted great attention because of their sensitive response to some trace ions and molecules. For example, diethyldithiocarbamate-functionalized CdSe/CdS QDs have been used as a fluorescent probe for copper ion detection,[22] manganese oxide QDs have been applied as a fluorescent probe for the detection of metal ions in aqueous media,[23] and carbon dots have been used as fluorescent probes for "off–on" detection of Cu^{2+} and L-cysteine in aqueous solutions.[24] However, agglomeration of these QDs can easily occur during their preparation and preservation as well as application because of their high surface energies, making them unstable. In addition, their PLs are easily affected by many external factors. As a result, their fluorescence properties change very easily.

In this study, we develop a luminescent nanomaterial with wide-wavelength response and good stability for use as a PL probe in aqueous solutions. Specifically, a novel open core–shell nanostructure, rod-Y_2O_3:Eu^{3+}@0.01YVO_4:Eu^{3+}, was designed and prepared, in which the core was partially coated with a quantum shell. In the open nanostructure proposed in this paper, the quantum shell plays a key role in the sensitivity of the material to trace ions.

2. Experimental section

2.1 Synthesis process

All the chemical reagents were analytical grade. Aqueous solutions of the precursors, $Y(NO_3)_3$ and $Eu(NO_3)_3$, were obtained by dissolving 1.061 g of Y_2O_3 and 0.0105 g of Eu_2O_3 (99.99%) in dilute HNO_3, and the resulting mixtures were then heated to remove excess HNO_3 solution. Next, 2 mol L^{-1} of NaOH solutions were used to adjust the pH of the above mixtures to 9. Finally, 0.0110 g of NH_4VO_3 (molar ratio $n_V : n_Y = 0.01$) was dispersed into the above suspensions, which were then subjected to ultrasonication for 15 min. The prepared precursor solutions were then transferred to a 100 mL autoclave and heated at 180 °C for 24 h. After cooling, the sample was collected, washed several times with water and ethanol, dried at 60 °C, and then annealed at 800 °C for 3 h. The final sample was identified as the partially coated core@shell rod-Y_2O_3:Eu^{3+}@0.01YVO_4:Eu^{3+}.

2.2 Fabrication and measurement of Cu^{2+} (off) and amino acid (on) sensor

Rod-Y_2O_3:Eu^{3+}@0.01YVO_4:Eu^{3+} (5 mL, 0.03 mg mL^{-1}) was placed in a centrifugal tube. Then, $Cu(NO_3)_2$ was also added to the container, giving a final concentration of Cu^{2+} ranging from 10^{-4} to 10^{-10} mol L^{-1}. After shaking well, the fluorescence spectra of the solutions were monitored under excitation at 280 nm.

For the detection of amino acids, 10^{-8} M of Cu^{2+} was added to rod-Y_2O_3:Eu^{3+}@0.01YVO_4:Eu^{3+} (5 mL, 0.03 mg mL^{-1}) to form a mixed solution, which was denoted as rod-Y_2O_3:Eu^{3+}@0.01YVO_4:Eu^{3+}–Cu^{2+} (10^{-8} mol L^{-1}). Amino acid was then added, with the final concentration of amino acid ranging from 0 to 1.0 × 10^{-8} mol L^{-1}. After shaking well, the fluorescence spectra of the solutions were monitored under excitation at 280 nm.

2.3 Characterization

The X-ray diffraction (XRD) patterns of the prepared samples were examined on an X-ray powder diffractometer (AXSD8-Advance, Bruker Company, Germany) with Cu Kα radiation ($\lambda = 0.15418$ nm, 40 kV, 30 mA). The Fourier transform infrared spectroscopy (FTIR) spectra were recorded on a Nicolet (Impact 410) infrared spectrophotometer using KBr pellets over the range of 400–4000 cm^{-1}. The morphologies of the samples were observed using scanning electron microscopy (SEM) (ZEISS ULTRA 55, Carl Zeiss NTS GmbH, Germany) and high-resolution transmission electron microscopy (HR-TEM, JEOL JEM-2100HR, Japan). The excitation and emission spectra were taken on Hitachi F-4600 spectrofluorometer equipped with a 150 W xenon lamp as the excitation source. All the measurements were performed at room temperature.

3. Results and discussion

3.1 Structural and morphological properties of rod-Y_2O_3:Eu^{3+}@0.01YVO_4:Eu^{3+} nanoparticles

XRD. The XRD pattern of the partially coated rod-Y_2O_3:Eu^{3+}@0.01YVO_4:Eu^{3+} nanostructure was collected, as shown in Fig. 1, and all of the XRD diffraction peaks can be readily indexed to the cubic structure of Y_2O_3 and the tetragonal structure of YVO_4, in accordance with the JCPDS cards 41-1105 and 17-0341. No additional diffraction peaks were observed, showing that there were no other impurities in this sample.

FT-IR. The FTIR spectra of pure Y_2O_3:Eu^{3+} and rod-Y_2O_3:Eu^{3+}@0.01YVO_4:Eu^{3+} are exhibited in Fig. 2. As shown in Fig. 2a, absorption peaks at 3441, 1520, 1410, and 560 cm^{-1} can be clearly observed in the spectrum of Y_2O_3:Eu^{3+}. A broad peak can also be seen at 3441 cm^{-1} due to the stretching mode of the hydroxyl groups.[25,26] Meanwhile, the typical absorption peak

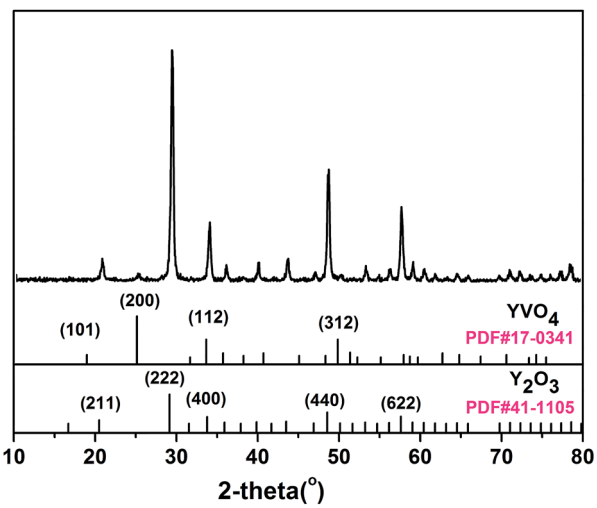

Fig. 1 XRD pattern of rod-Y_2O_3:Eu^{3+}@0.01YVO_4:Eu^{3+}.

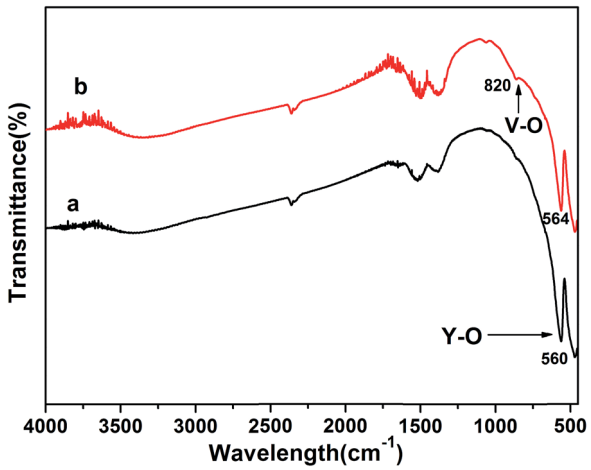

Fig. 2 FT-IR spectra of pure Y_2O_3:Eu^{3+} (a) and rod-Y_2O_3:-Eu^{3+}@0.01YVO_4:Eu^{3+} (b).

corresponding to the Y–O stretching vibration of Y_2O_3 is present at 560 cm^{-1}.[27] Furthermore, a new vibration peak can be seen in Fig. 2b at 821 cm^{-1}, which can be attributed to the V–O stretching vibration in the VO_4^{3-} tetrahedron.[28] The FT-IR spectra reveal clearly that Y_2O_3:Eu^{3+} and YVO_4:Eu^{3+} co-existed in the prepared nanocomposite.

SEM, EDS, and HR-TEM. The morphology of rod-Y_2O_3:-Eu^{3+}@0.01YVO_4:Eu^{3+} is exhibited in Fig. 3. The particles were uniform and monodispersed rods, with an average diameter of ~50 nm and a length of ~400 nm. In order to determine the chemical composition of the rod-Y_2O_3:Eu^{3+}@0.01YVO_4:Eu^{3+}, EDS measurement was performed on the area of the material SEM in Fig. 4. The EDS analysis indicated that the main composition of the nanorods is yttrium and oxygen. Small amount of vanadium and europium were also detected. These results indicated that the chemical composition of the rod-Y_2O_3:Eu^{3+}@0.01YVO_4:Eu^{3+} is uniform.

Furthermore, the rod-Y_2O_3:Eu^{3+}@0.01YVO_4:Eu^{3+} was examined by TEM and HR-TEM in order to verify its partially coated structure, as displayed in Fig. 5. The composite structure of the rod-Y_2O_3:Eu^{3+}@0.01YVO_4:Eu^{3+} was investigated with a HRTEM, some breaking areas could be found on the rod and it exhibited a discontinuous interface. As shown in Fig. 5b1, the measured lattice spacing of the nanorod was 0.35 nm, indicating a (200) crystal growth direction and a SAED pattern recorded (left) from the same area, which confirmed that the nanorod is single crystalline and indicated that the growth direction is (200) of YVO_4:Eu^{3+}.[9] Therefore, a lattice spacing of the crystalline can be identified 0.29 nm (222) crystal growth direction of Y_2O_3:Eu^{3+} in Fig. 5b2.[29] Obviously, the partially coated structure had been successfully synthesized, while the YVO_4:Eu^{3+} shell partially covered the Y_2O_3:Eu^{3+} core with a size less than 5 nm, similar emission property expected to that of a typical quantum dot.

PL. The excitation spectra of pure Y_2O_3:Eu^{3+} (a), pure YVO_4:Eu^{3+} (b), and rod-Y_2O_3:Eu^{3+}@0.01YVO_4:Eu^{3+} (c) are shown in Fig. 6 (left). Only one peak appeared for pure Y_2O_3:Eu^{3+}, at 254 nm, which corresponded to the charge-transfer band (CTB) related to an electronic transition from the 2p orbital of O^{2-} to

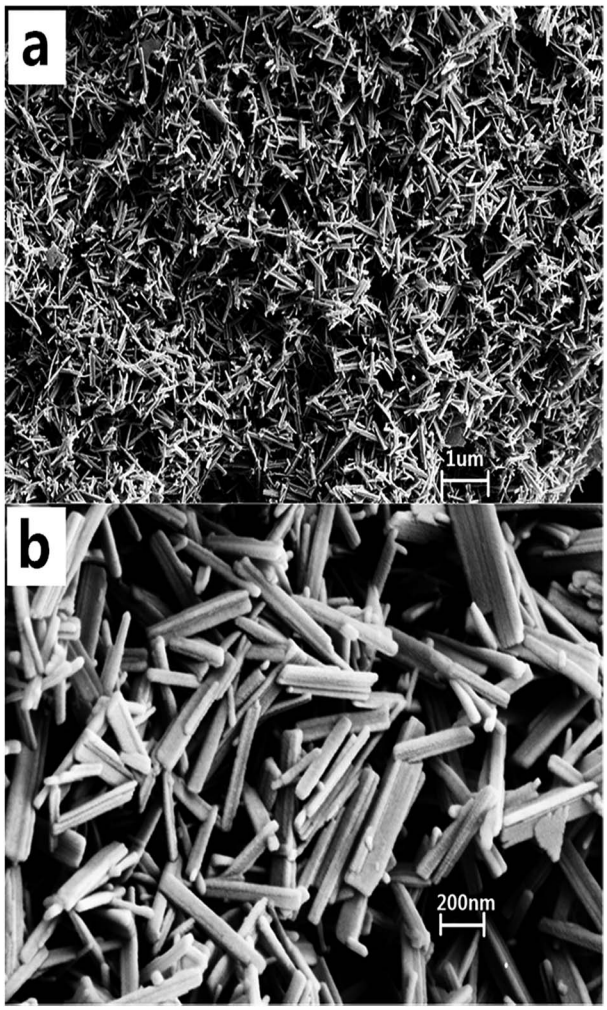

Fig. 3 SEM images of rod-Y_2O_3:Eu^{3+}@0.01YVO_4:Eu^{3+}.

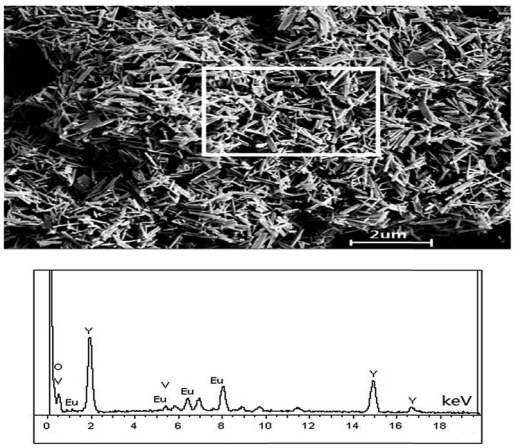

Fig. 4 A SEM image of as-prepared nanorods (up) with collection area marked, and EDX signals (down, EDS spectrum).

the 4f orbital of Eu^{3+}.[30] Pure YVO_4:Eu^{3+} also only possessed one excitation band, at 308 nm, which can be regarded as a charge transfer from the O atoms of the ligands to the central V atom

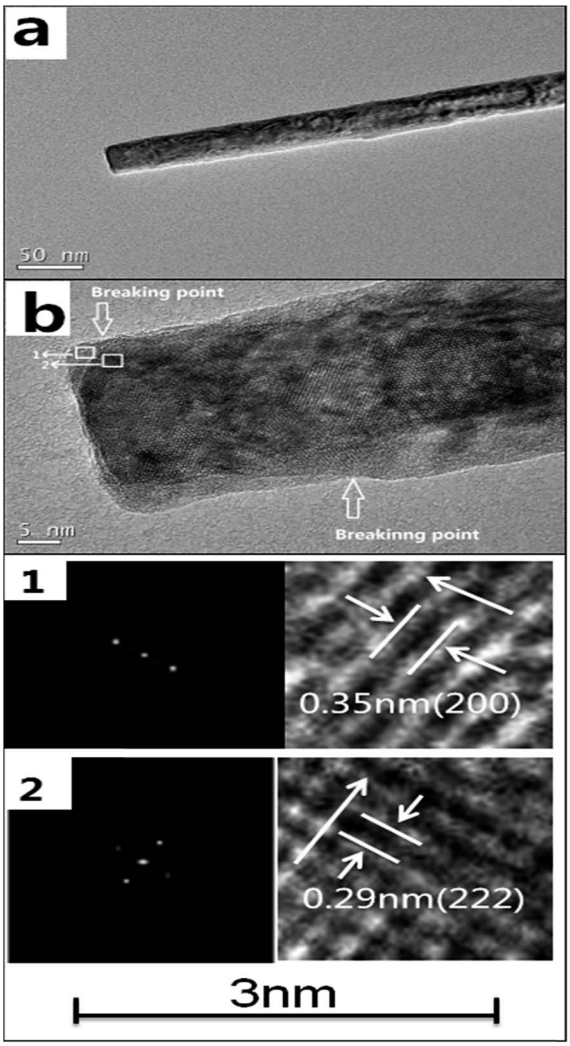

Fig. 5 TEM (a) and HRTEM (b) images of rod-Y_2O_3:Eu^{3+}@0.01YVO_4:Eu^{3+} (b1, b2: representative SAED patterns and the measured lattice spacing of the crystalline).

inside the VO_4^{3-} group.[31] However, the spectrum of rod-Y_2O_3:Eu^{3+}@0.01YVO_4:Eu^{3+} contained a broader excitation band in the range of 200–350 nm, which can be seen as two peaks centered at ~254 nm and ~280 nm, similar to that of a ~5 nm YVO_4:Eu^{3+} quantum dot layer, albeit slightly blue-shifted.[32] The former peak was likely related to the CTB in Y_2O_3:Eu^{3+}, while the latter corresponded to a vanadate band in the open quantum shell of YVO_4:Eu^{3+}. This special optical property is only observed in partially coated core/shell structures, and cannot be replicated in fully coated core/shell materials. In order to show this, a sample was prepared with more NH_4VO_3, corresponding to a V/Y molar ratio of 0.4. SEM and HR-TEM images of the nanocomposite prepared with 0.436 g of NH_4VO_3 (molar ratio $n_V : n_Y = 0.4$) are shown in Fig. S1 (see ESI†). The HR-TEM image shows that a continuous interface can be clearly observed, meaning that the shell of YVO_4:Eu^{3+} had totally covered the surface of the core Y_2O_3:Eu^{3+}. The excitation spectrum of this material is shown in Fig. S2.† Surprisingly, the full coated sample showed only one excitation band at 308 nm,

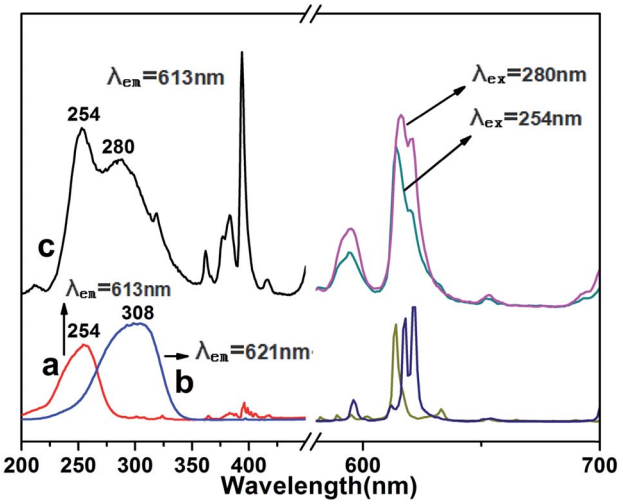

Fig. 6 Excitation (left) and emission (right) spectra of pure Y_2O_3:Eu^{3+} (a), pure YVO_4:Eu^{3+} (b), and rod-Y_2O_3:Eu^{3+}@0.01YVO_4:Eu^{3+} (c).

corresponding to that of YVO_4:Eu^{3+}. The continuous shell fully encompassed the core, enhancing the transition competition between the shell and the core. It can be concluded that efficient energy transfer from Y_2O_3:Eu^{3+} to YVO_4:Eu^{3+} occurred following the excitation into the CTB of Y_2O_3:Eu^{3+}.[33] Therefore, the novel nanostructure rod-Y_2O_3:Eu^{3+}@0.01YVO_4:Eu^{3+}, in which YVO_4:Eu^{3+} was only partially coated on the Y_2O_3:Eu^{3+} core, acted as a smart phosphor which exhibited PL under wide-band excitation covering the range of 200–350 nm, as displayed in Fig. 6. This wide-band response phosphor emitted strong red light, and may be a candidate as a fluorescent probe for use in chemical and biological detection.

Cu^{2+} (off) and amino acid (on) sensing characteristics of rod-Y_2O_3:Eu^{3+}@0.01YVO_4:Eu^{3+} nanoparticles. The fluorescence quenching that occurs upon the addition of Cu^{2+} can be observed in Fig. 7, which shows the fluorescence intensity of the partially coated rod-Y_2O_3:Eu^{3+}@0.01YVO_4:Eu^{3+} decreasing

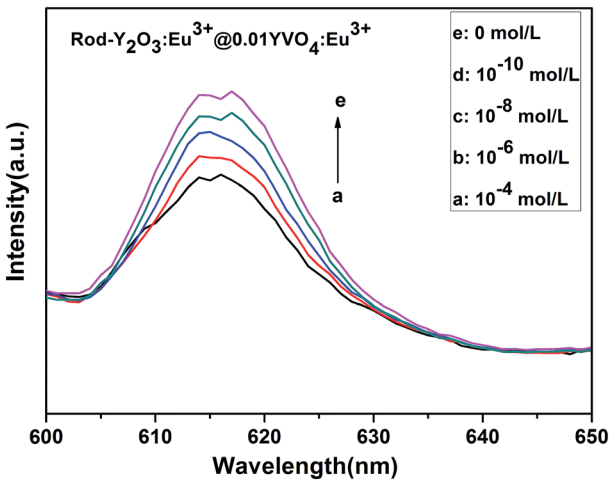

Fig. 7 Fluorescence response of rodY_2O_3:Eu^{3+}@0.01YVO_4:Eu^{3+} in the presence of increasing concentration of Cu^{2+}.

gradually as the Cu^{2+} concentration was increased. Meanwhile, pure Y_2O_3:Eu^{3+} (Fig. S3†), pure YVO_4:Eu^{3+} (Fig. S4†), Y_2O_3:Eu^{3+} coated with 0.01YVO_4:Eu^{3+} by physical blending (Fig. S5†), and fully coated Y_2O_3:Eu^{3+}@0.4YVO_4:Eu^{3+} (Fig. S6†) were exposed to the same conditions to illustrate the excellent properties of the partially coated structure. Fig. 8 shows that the partially coated rod-Y_2O_3:Eu^{3+}@0.01YVO_4:Eu^{3+} had a linear relationship with the Cu^{2+} concentration (linear regression equation: $y = 0.0396x + 0.5655$, $R^2 = 0.9962$), with the fluorescence intensity decreasing with increasing concentration of Cu^{2+}. However, there were no obvious linear relationships between the concentration of Cu^{2+} and the other four materials. The partially coated nanostructures were also tested in the presence of 2, 4, 6, and 8 × 10^{-8} mol L^{-1} (Fig. S7†) and 2, 4, 6, and 8 × 10^{-10} mol L^{-1} (Fig. S8†) of Cu^{2+}. Good linear relationships were also observed for these Cu(II) concentrations. In Fig. 9, I and I_0 are the fluorescence intensities of Y_2O_3:Eu^{3+}@0.01YVO_4:Eu^{3+} in the presence and absence of Cu^{2+}, respectively. Linear regression equations can be obtained for I/I_0 under these conditions, which are $y = -1.4175x + 85.365$, $R^2 = 0.9947$ ((a): 2, 4, 6, 8 × 10^{-8} mol L^{-1} grads) and $y = -1.076x + 93.51$, $R^2 = 0.9954$ ((b): 2, 4, 6, 8 × 10^{-10} mol L^{-1} grads).

This shows that the partially coated rod-Y_2O_3:Eu^{3+}@0.01YVO_4:Eu^{3+} nanostructures possess excellent properties that make them suitable for use as a fluorescent probe for the detection of Cu(II) ions. Quantum dots are already frequently used for the detection of minute quantities of elements. The partial YVO_4:Eu^{3+} shells are as thin as quantum dots are small, providing outstanding properties that enable the detection of minute quantities of elements *via* use as a fluorescent probe. The emission intensity of the rod-Y_2O_3:Eu^{3+}@0.01YVO_4:Eu^{3+} decreased as the concentration of Cu(II) ions increased. Thus, a fluorescently quenched probe (off state) was obtained.

The quenching (off) of the rod-Y_2O_3:Eu^{3+}@0.01YVO_4:Eu^{3+}–Cu^{2+} (10^{-8} mol L^{-1}) system can be explored as a new fluorescent probe for the detection of amino acids based on the competition mechanism between amino acids, Cu^{2+}, and rod-Y_2O_3:Eu^{3+}@0.01YVO_4:Eu^{3+}. Glutamic acid and leucine were employed to illustrate this principle. The fluorescence spectra of rod-Y_2O_3:Eu^{3+}@0.01YVO_4:Eu^{3+}–Cu^{2+} (10^{-8} mol L^{-1}) with glutamic acid (Fig. S9†) and leucine (Fig. S10†) were measured, and the relationships between the fluorescence intensities of the rod-Y_2O_3:Eu^{3+}@0.01YVO_4:Eu^{3+}–Cu^{2+} and the concentrations of the amino acids are shown in Fig. 10 (glutamic acid) and Fig. 11 (leucine). The linear regression equations ($y = 111.85 + 24.98x$, $R^2 = 0.9982$ (glutamic acid) and $y = 248.40 + 19.96x$, $R^2 = 0.9986$ (leucine)) indicate that the rod-Y_2O_3:Eu^{3+}@0.01YVO_4:Eu^{3+}–Cu^{2+} (10^{-8} mol L^{-1}) system can be used as a fluorescent probe for amino acids, as the fluorescence intensities of these samples increased with the concentration of amino acids, as the fluorescence intensity of the sample was restored (on state).

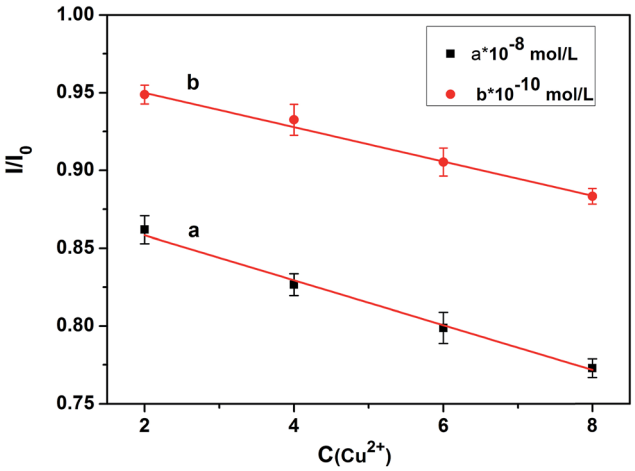

Fig. 9 Linear I/I_0 relationships *versus* concentration of Cu^{2+} over the ranges of 2–8 × 10^{-8} mol L^{-1} and 2–8 × 10^{-10} mol L^{-1}, respectively. The error bars represent the standard deviations of three measurements.

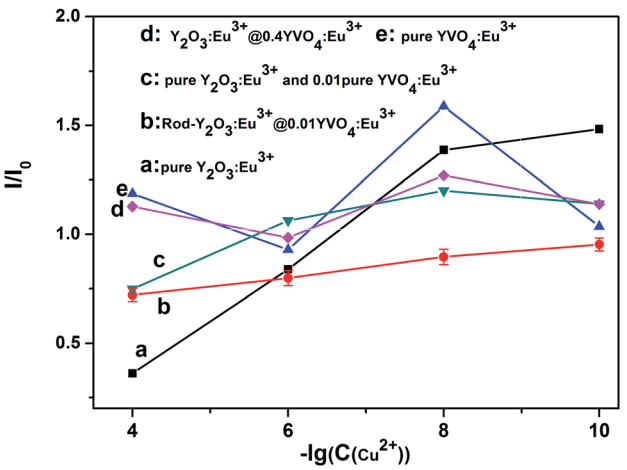

Fig. 8 I/I_0 relationships of five different samples with increasing Cu^{2+} concentration.

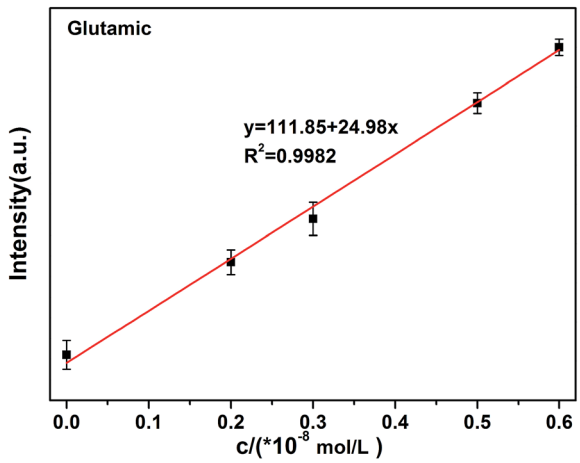

Fig. 10 Linear relationship of the fluorescence intensity *versus* the concentration of glutamic acid over the range of 0–1.0 × 10^{-8} mol L^{-1}. The error bars represent the standard deviations of three measurements.

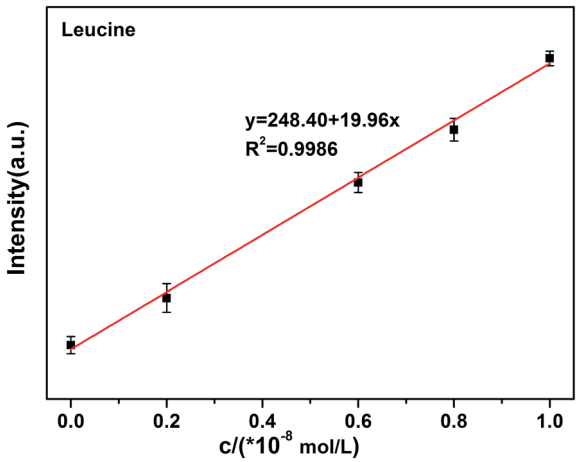

Fig. 11 Linear relationship of the fluorescence intensity *versus* the concentration of leucine over the range of 0–1.0 × 10^{-8} mol L^{-1}. The error bars represent the standard deviations of three measurements.

The mechanism of the "off-and-on" detection of Cu^{2+} and amino acids using anisotropic rods of Y_2O_3:Eu^{3+} that were partially coated with 0.01YVO_4:Eu^{3+} as fluorescent probes is shown in Scheme 1. There were many –OH groups on the surface of the YVO_4:Eu^{3+} quantum shell in the rod-Y_2O_3:Eu^{3+}@0.01YVO_4:Eu^{3+} composite nanostructure while dispersed in aqueous solution, which can easily combine with Cu^{2+} to form $[Cu(OH)_4]^-$. As is well known, $[Cu(OH)_4]^-$ ions appear blue in aqueous solutions due to their absorption of red light, while the rod-Y_2O_3:Eu^{3+}@0.01YVO_4:Eu^{3+} nanocomposite is a red phosphor when excited with UV light. Therefore, the fluorescence intensity of the rod-Y_2O_3:Eu^{3+}@0.01YVO_4:Eu^{3+} nanocomposite was reduced or even quenched in the presence of trace Cu^{2+}, allowing this OCSNS to be used as a probe for the detection of Cu^{2+}. On other hand, the fluorescence intensity of the rod-Y_2O_3:Eu^{3+}@0.01YVO_4:Eu^{3+}–Cu^{2+} (10^{-8} mol L^{-1}) system was increased in the presence of trace amino acids. The amino acids possess a strong binding preference toward Cu^{2+}, which removed Cu^{2+} from the surface of the partially coated nanocomposite, thus decreasing the concentration of $[Cu(OH)_4]^-$ and allowing the fluorescence of the system to recover. The opposite fluorescent responses in the presence of Cu^{2+} and amino acids give this rod-Y_2O_3:Eu^{3+}@0.01YVO_4:Eu^{3+} OCSNS the potential to be used to detect trace Cu^{2+} and amino acids, exhibiting "off-and-on" fluorescence properties.

Scheme 1 Schematic illustration of Cu^{2+} and amino acid detection using rod-Y_2O_3:Eu^{3+}@0.01YVO_4:Eu^{3+}.

4. Conclusions

In conclusion, partially coated core–shell nanostructures, rod-Y_2O_3:Eu^{3+}@0.01YVO_4:Eu^{3+}, were first fabricated by a facile hydrothermal approach. The crystal structure, morphology, and optical properties were characterized in detail by XRD, FTIR, SEM, TEM, and PL spectroscopy. This revealed that a quantum shell of YVO_4:Eu^{3+} had been partially coated onto the surfaces of the Y_2O_3:Eu^{3+} core. The excitation spectra of this special nanostructure can be deconstructed into two components centered at ~254 and ~280 nm, covering a much wider excitation period of UV wavelengths than is obtained for either material alone. Other OCSNSs composed of an anisotropic core or substrate and an open shell with a thickness of less than 5 nm can also be fabricated in the same way, and the photoluminescent performances of these materials in the presence of trace ions or molecules can be examined. As an example, super sensitive probes consisting of rod-Y_2O_3:Eu^{3+}@0.01YVO_4:Eu^{3+} with "off-and-on" properties can be employed to detect minute amounts of Cu(II) ions (off), followed by reuse as a fluorescent probe for various amino acids (on). Far more examples of this kind of OCSNS, their probing properties, and their selectivity performances will be examined in the future for the purpose of inventing novel fluorescent probes.

Conflicts of interest

There are no conflicts to declare.

Acknowledgements

The authors acknowledge the financial support from the National Natural Science Foundation of China (Grant No. 11374109) and the Natural Science Foundation of Guangdong Province, China (Grant. No. 2016A030308010). S. Lan and S. Tie would like to thank the financial support from the Science and Technology Planning Project of Guangdong Province, China(Grant No. 2015B090927006).

References

1 D. Y. Fan, S. Yang, J. Q. Wang, A. Q. Zheng, X. P. Song and D. M. Yu, *J. Lumin.*, 2012, **132**, 1122–1125.
2 S. J. Wang, J. B. Hu, Y. Y. Wang and F. Luo, *J. Mater. Sci.*, 2013, **48**, 805–811.
3 S. Zhang, H. B. Liang, C. M. Liu, Z. M. Qi, T. Shao and Y. Y. Wang, *Opt. Lett.*, 2013, **38**, 612–614.
4 S. L. Gai, C. X. Li, P. P. Yang and J. Lin, *Chem. Rev.*, 2014, **114**, 2343–2389.
5 G. C. Li, M. Lv, J. Dai and X. Li, *Opt. Mater.*, 2015, **46**, 40–44.
6 A. Khanna and P. S. Dutta, *J. Solid State Chem.*, 2013, **198**, 93–100.

7 P. Gupta, A. K. Bedyal, V. Kumar, Y. Khajuria, V. Kumar, E. Coetsee-Hugo, O. M. Ntwaeaborwa and H. C. Swart, *Opt. Mater.*, 2014, **36**, 996–1001.
8 D. den Engelsen, G. R. Fern, T. G. Ireland, P. G. Harris, P. R. Hobson, A. Lipman, R. Dhillon, P. J. Marsha and J. Silver, *J. Mater. Chem. C*, 2016, **4**, 7026–7034.
9 L. Zhu, J. Y. Li, Q. Li, X. D. Liu, J. Meng and X. Q. Cao, *Nanotechnology*, 2007, **18**, 055604.
10 W. X. Wang, Z. Y. Cheng, P. P. Yang, Z. Y. Hou, C. X. Li, G. G. Li, Y. L. Dai and J. Lin, *Adv. Funct. Mater.*, 2011, **21**, 456–463.
11 T. Liu, W. Xu, X. Bai and H. W. Song, *J. Appl. Physiol.*, 2012, **111**, 064312.
12 K. Kömpe, H. Borchert, J. Storz, A. Lobo, S. Adam, T. Möller and M. Haase, *Angew. Chem., Int. Ed. Engl.*, 2003, **42**, 5513–5516.
13 H. Wang, M. Yu, C. K. Lin and J. Lin, *J. Colloid Interface Sci.*, 2006, **300**, 176–182.
14 W. T. Gan, S. L. Xiao, L. K. Gao, R. A. Gao, J. Li and X. X. Zhan, *ACS Sustainable Chem. Eng.*, 2017, **5**, 3855–3862.
15 M. L. Chang and S. L. Tie, *Nanotechnology*, 2008, **19**, 075711.
16 Z. Wu, L. Lin, W. Yang, D. Zhang, C. Shen, W. Lou, H. Yin and K. Chang, *RSC Adv.*, 2017, **7**, 30963–30969.
17 M. Jing, J. Wang, H. Hou, Y. Yang, Y. Zhang, C. Pan, J. Chen, Y. Zhu and X. Ji, *J. Mater. Chem. A*, 2015, **3**, 16824–16830.
18 L. C. Spangler, L. Lu, C. Kiely, B. W. Berger and S. McIntosh, *J. Mater. Chem. A*, 2016, **4**, 6107–6115.
19 M. Zeng, X. Peng, J. Liao, G. Wang, Y. Li, J. Li, Y. Qin, J. Wilson, A. song and S. Lin, *Phys. Chem. Chem. Phys.*, 2016, **18**(26), 17404.
20 P. O. Anikeeva, J. E. Halpert, M. G. Bawendi and V. Bulović, *Nano Lett.*, 2009, **9**, 2532–2536.
21 B. A. Kairdolf, A. M. Smith, T. H. Stokes, M. D. Wang, A. N. Young and S. M. Nie, *Annu. Rev. Anal. Chem.*, 2013, **6**, 143–162.
22 J. Z. Wang, X. P. Zhou, H. B. Ma and G. H. Tao, *Spectrochim. Acta, Part A*, 2011, **81**, 178–183.
23 S. Rong, P. Zhang, Y. Yang and F. Liu, *RSC Adv.*, 2016, **6**, 114632–114638.
24 J. Zong, X. L. Yang, A. Trinchi, S. Hardin, I. Cole, Y. H. Zhu, C. Z. Li, T. Muster and G. Wei, *Biosens. Bioelectron.*, 2014, **51**, 330–335.
25 P. Jeevanandam, Y. Koltypin, O. Palchik and A. Gedanken, *J. Mater. Chem.*, 2001, **11**, 869–873.
26 N. Venkatachalam, Y. Saito and K. Soga, *J. Mater. Chem.*, 2001, **11**, 869–873.
27 X. Y. Shen and Y. C. Zhai, *Rare Met.*, 2011, **30**, 33–38.
28 Y. J. Liang, J. Ouyang, H. Y. Wang, W. L. Wang, P. F. Chui and K. N. Sun, *Appl. Surf. Sci.*, 2012, **258**, 3689–3694.
29 R. J. Gaboriaud, F. Pailloux, P. Guerin and F. Paumier, *J. Phys. D: Appl. Phys.*, 2000, **33**, 2884–2889.
30 H. Razavi-Khosroshahi, K. Edalati, H. Emami, E. Akiba, Z. Horita and M. Fuji, *Inorg. Chem.*, 2017, **56**, 2576–2580.
31 A. M. Kaczmarek, D. Ndagsi and R. Van Deun, *Dalton Trans.*, 2016, **45**, 16231–16239.
32 A. F. Khan, D. Haranath, R. Yadav, S. Singh, S. Chawla and V. Dutta, *Appl. Phys. Lett.*, 2008, **93**, 073103.
33 G. H. Pan, H. W. Song, X. Bai, Z. G. Liu, H. Q. Yu, W. H. Di, S. W. Li, L. B. Fan, X. G. Ren and S. Z. Lu, *Chem. Mater.*, 2006, **18**, 4526–4532.